Journal of Orthopaedic Research®

WILEY | ORS Orthopaedic Research Society

RESEARCH ARTICLE OPEN ACCESS

Molecular Mechanisms of Rotator Cuff Degeneration Identified by Spatial Transcriptomics and Multiplex Immunofluorescence

Shiyi Yao[1] | Renhao Yang[1] | Shifeng Ling[2] | Gen Li[1] | Hanyu Wang[1] | Renxuan Li[1] | Yang Xu[1] | Yin Zhang[1] | Chengyu Zhuang[1] | Lei Wang[1]

[1]Clinical Center for Sports Medicine, Department of Orthopedics, Ruijin Hospital, Shanghai Jiao Tong University School of Medicine, Shanghai, China | [2]Department of Orthopedics, Shanghai Key Laboratory for Prevention and Treatment of Bone and Joint Diseases, Shanghai Institute of Traumatology and Orthopedics, Ruijin Hospital, Shanghai Jiao Tong University School of Medicine, Shanghai, China

Correspondence: Lei Wang (ray_wangs@hotmail.com)

Received: 11 September 2025 | **Revised:** 10 February 2026 | **Accepted:** 17 February 2026

Funding: National Natural Science Foundation of China, Grant/Award Numbers: 82402784, 82472419; Postdoctoral Science Foundation General Program, Grant/Award Number: 2024M762056

Keywords: multiplex immunofluorescence | rotator cuff tear | spatial transcriptomics

ABSTRACT

Rotator cuff tear (RCT) is a prevalent age-related condition whose underlying mechanisms remain poorly understood. This study employed spatial transcriptomics and multiplex immunofluorescence (mIF) to investigate gene expression and spatial heterogeneity in rotator cuff tissues from elderly RCT patients compared to age-matched controls, aiming to uncover key molecular pathways. Tendon samples were collected from RCT patients ($n = 10$) and controls ($n = 10$). Five from each group underwent spatial transcriptomic sequencing for differential gene expression, functional enrichment, and cell interaction analyzes. Results were validated with mIF on the remaining samples. Compared to controls, the RCT group showed 1261 downregulated and 2789 upregulated genes. Spatial analysis revealed distinct expression gradients: COMP and CHI3L1 were upregulated in the bone region, CHI3L1 and MT1X in the mid-tendon, and MT1X and FMOD in the tendon area—confirmed by mIF. Biological processes also varied regionally: cartilage development and extracellular matrix (ECM) organization were enriched in the bone, while ECM and collagen fibril organization dominated mid-tendon and tendon regions. The PI3K-AKT and ECM-receptor interaction pathways were central to these processes. Tenogenic progenitor-like cells (TPLCs) were significantly reduced in RCT ($p < 0.0001$), whereas mesenchymal cells increased in bone and mid-tendon areas ($p < 0.001$, $p < 0.01$), consistent with structural gradients. These findings suggest that elderly RCT may arise from chronic inflammation, ECM dysregulation, and failed regeneration. Spatial transcriptomics identified repair-related genes (COMP, CHI3L1, MT1X, FMOD) with region-specific expression, providing new insights into pathology and potential therapeutic targets.

1 | Introduction

Rotator cuff tear (RCT) is a common musculoskeletal disorder among the elderly, with an incidence rate exceeding 20% [1]. This disease is primarily characterized by persistent shoulder pain, limited joint mobility, and progressive muscle weakness [2]. In severe cases, it can lead to upper limb dysfunction [3] and significantly reduce the quality of life of patients. Although arthroscopy techniques and surgical repair methods have been

Shiyi Yao and Renhao Yang contribute equally to this work.

continuously improving in recent years, the rate of retear after surgery remains high (10%–48.4%) [4, 5], indicating that the current treatment strategies still have limitations in terms of efficacy. It is worth noting that some elderly people, even at an advanced age, can still maintain relatively healthy rotator cuff tissues [6]. These individual differences indicate the need for comprehensive research into the molecular mechanisms of RCT in the elderly. Clarifying these mechanisms not only aids in preventing the occurrence of RCT but also offers a theoretical foundation for developing new treatment methods and enhancing clinical outcomes, thereby possessing substantial scientific value and clinical significance.

Regarding the molecular mechanisms of RCT in the elderly, various technical approaches have provided multidimensional evidence. A study conducted in South Korea [7] analyzed the mRNA levels of 15 specimens, including 12 patients with RCT and 3 control specimens with proximal humeral fractures, using PCR. The results indicated that COL3A1 and COL10A1 exhibited a significant increasing trend, while COL4A1 and COL14A1 demonstrated a decreasing trend. Additionally, ACAN, FN1, and TNC were significantly elevated compared to the normal group, whereas DCN, LUM, ELN, LAMA2, and THBS1 showed a decreasing trend. Another study [8] utilized a genome-wide association study to demonstrate that, compared to the control group, the expression of the THSD7A gene was significantly downregulated in patients with rotator cuff tears, suggesting a potential functional role. Additionally, the tissue expressions of the TIMP2, Col5A1, TGFBR1, and TNC genes were significantly upregulated, further supporting the biological roles of these genes in the context of tears. Chaudhury et al. conducted microarray analysis on the gene expression profiles of 28 human rotator cuff tendons [9], which included 11 cases of large tears, 5 cases of small tears, and 12 age-matched normal control specimens. The results indicated that rotator cuff tears exhibited upregulated expression of several matrix metalloproteinases (MMPs), including MMP-3, MMP-10, MMP-12, MMP-13, MMP-15, MMP-21, and MMP-25. Additionally, there was an upregulation of the disintegrin and metalloproteinase (ADAM) genes, especially ADAM-12, ADAM-15, and ADAM-22, alongside a downregulation of certain interleukins (IL-1, IL-8, and IL-27), which play crucial roles in chemotaxis. Robert et al. [10] employed RNA sequencing to compare the RCT samples from 24 patients with those from 9 control subjects. They discovered that the expression of hypoxia-related target genes was elevated in minor, less contracted tears, which promoted wound healing. In contrast, larger, more contracted tears were associated with endothelial cell markers and resulted in poor healing outcomes. Most recently, published by Fu et al., datasets from human rotator cuff tendon tissues revealed changes in cell heterogeneity during progression of human tendinopathy [11]. These findings have provided a valuable molecular framework for understanding age-related RCT. However, they do not account for the spatial heterogeneity of the degenerative patterns observed in clinical practice. Furthermore, the gene expression characteristics cannot yet be comprehensively analyzed.

Digital spatial profiling (DSP) [12] is an advanced technology specifically designed for conducting high-resolution analyzes of proteins and RNA in tissue samples. This technology integrates spatial analysis with molecular analysis, enabling researchers to gain a deeper understanding of tissue structure and intercellular interactions [13]. Additionally, multiplex immunofluorescence (mIF) [14] is a complex technique mainly used in biological and medical research to visualize multiple antigens within a single sample. This method leverages the unique properties of fluorescent dyes attached to antibodies, enabling the simultaneous detection of multiple targets within tissues or cells [15].

In this study, we integrated DSP analysis and mIF techniques to investigate the molecular profiles of tears in various regions of the rotator cuff in elderly individuals. This approach allowed us to elucidate the potential roles of these molecules in the rotator cuff and to identify the possible interaction patterns among them, thereby revealing potential mechanisms and therapeutic targets involved in the injury and healing processes.

2 | Methods

2.1 | Specimen Collection

This study received approval from the Ethics Committee of Ruijin Hospital, Shanghai Jiao Tong University School of Medicine (Shanghai, China; No. 2024-53). All donors (with symptoms 3 to 6 months before the operation) provided written informed consent for the use of their excised rotator cuff tissue (supraspinatus). They were fully informed about the purpose of the research, and no compensation was offered for their donations.

Twenty paraffin sections of human rotator cuff tendon tissue (10 for DSP and 10 for mIF, selected as adjacent sections from the same tissue blocks) were meticulously dissected from 20 donors in this study (see Table 1). Tissue samples from patients undergoing rotator cuff repair were categorized into the RCT group, while tissue from patients undergoing shoulder joint replacement was classified as the control group.

2.2 | DSP Analysis

DSP was conducted following previously published methods (GeoMx DSP, Nanostring, sequencing depth calculation: number of read pairs = total collection area (μm^2) x 100) [12]. Briefly, after the slides were deparaffinized and subjected to antigen retrieval procedures, the samples were co-incubated with fluorescently labeled visualization antibodies (for detailed antibody information, see Table 2) to detect tenogenic progenitor cells (SCX), macrophages (CD68), and fibroblasts (α-SMA), along with DAPI for nuclei detection. Customizable fluorescent morphology markers, conjugated to unique oligonucleotide tags with an ultraviolet (UV) photocleavable linker, facilitated the visualization of the tissue architecture. The samples were imaged, and regions of interest (ROIs) were exposed to UV light, which cleaved the linker and released the barcoded oligonucleotides for capture by microfluidics. The GeoMx DSP was then coupled with next-generation sequencing (NGS) to profile RNA expression, enabling the identification of over 18,000 genes in the samples.

2.3 | Quality Control (QC) of DSP

The GeoMx transcriptomic data were analyzed using the R software package standR (v1.7.4). Quality control was performed following data import. By default, genes present in

TABLE 1 | Cinicopathological characteristics of RCT/Control patients.

Characteristics	Control sample [DSP, $n = 5$]	RCT sample [DSP, $n = 5$]	Control sample [mIF, $n = 5$]	RCT sample [mIF, $n = 5$]
Sex [n, (%)]				
Male	3 (60%)	2 (40%)	1 (20%)	1 (20%)
Female	2 (40%)	3 (60%)	4 (80%)	4 (80%)
Age [n, (%)]				
< = 70	2 (40%)	2 (40%)	1 (20%)	1 (20%)
> 70	3 (60%)	3 (60%)	4 (80%)	4 (80%)
The reason for the surgery	4 Proximal humerus fracture 1 Shoulder arthritis	RCT	3 Proximal humerus fracture 2 Shoulder arthritis	RCT

TABLE 2 | The detailed information of the antibodies used.

Antibody name	Manufacturer	Product code	Specification
SCX	Abcam	Ab58655	1:100
CD68	ZSGB-Bio	ZM-0060	1:100
α-SMA	NOVUS-Bio	NBP2-34522AF647	1:400
COMP (Anti-COMP/Cartilage oligomeric matrix)	Abcam	ab231977	1:100
MT1X (MT1X Polyclonal antibody)	Proteintech	17172-1-AP	1:400
CHI3L1 (CHI3L1/YKL40 Polyclonal antibody)	Proteintech	12036-1-AP	1:200
FMOD (Fibromodulin Monoclonal antibody)	Proteintech	60108-1-Ig	1:800

fewer than 90% of the samples and with counts less than 5 were excluded. Low-quality areas of interest (AOIs) with relatively small library sizes and low cell counts were also removed, with a threshold set at an AOI Nuclei Count greater than 5. Batch effect removal was performed using the geomx Batch Correction function in conjunction with the RUV4 correction method (k = 3). Normalization was executed using the geomx Norm function in standR, employing the TMM (Trimmed Mean of M-values) method [16].

2.4 | Spatial Transcriptomic Data Analysis

Differential expression analysis was conducted using the R software package limma (v3.50.3). Genes were classified as differentially expressed based on the following threshold criteria: p-value < 0.05 and |log2FC | ≥ 0. In order to evaluate the functions of the genes of interest identified in the study, the R package ClusterProfiler (v4.4.4) was utilized with default settings for enrichment analysis of datasets, including Gene Ontology, KEGG, and MSigDB (hallmark gene sets). The Benjamini-Hochberg method was employed to correct for multiple testing. The top 20 enrichment items and pathways, listed in ascending order of p-value, were selected for visualization. The CIBERSORT method was utilized to infer the cell composition involved within the study area based on the expression data from the scRNA datasets (GSE223751, GSE182997).

2.5 | mIF Assay

5 control rotator cuff samples and 5 RCT samples were subjected to mIF staining. Slides, each 5 μm, were cut from FFPE blocks were dewaxed with xylene, and rehydrated through a decreasing series of ethanol concentrations. The samples were then fixed in 10% neutral buffered formalin for 10 min. Antigen retrieval was performed using a pressure cooker for 20 min. Subsequently, the tissue sections were stained with 4 antibodies for 3 h (see Table 2). For the target antigens, we selected representative markers based on the sequencing results. The selected markers include COMP (abcam, ab231977), FMOD (proteintech, 60108-1-Ig), MT1X (proteintech, 17172-1-AP), and CHI3L1 (proteintech, 12036-1-AP). Imaging analysis was performed using HALO image analysis software (version v3.4.2986.235, Indica Labs Inc.).

3 | Result

3.1 | Experimental Procedure and General Morphology

To ensure comparability, the demographic characteristics of the control group were similar to those of the RCT patients. The majority of patients were female (65%), and the majority were over 70 years old (70%). Among the 10 RCT patients, 7 had proximal humeral fractures, while the remaining 3 suffered from severe shoulder arthritis (see Table 1). Tissue samples from 5 RCT patients and 5 control group participants underwent advanced DSP analysis, while the remaining specimens were analyzed using mIF based on the DSP results (Figure 1A). The gross sections and staining of the control group indicated that the specimens generally exhibited a dense connective tissue morphology (Figure 1B(a)), characterized by neatly arranged fibers and cells in the HE sections. In contrast, the tissue

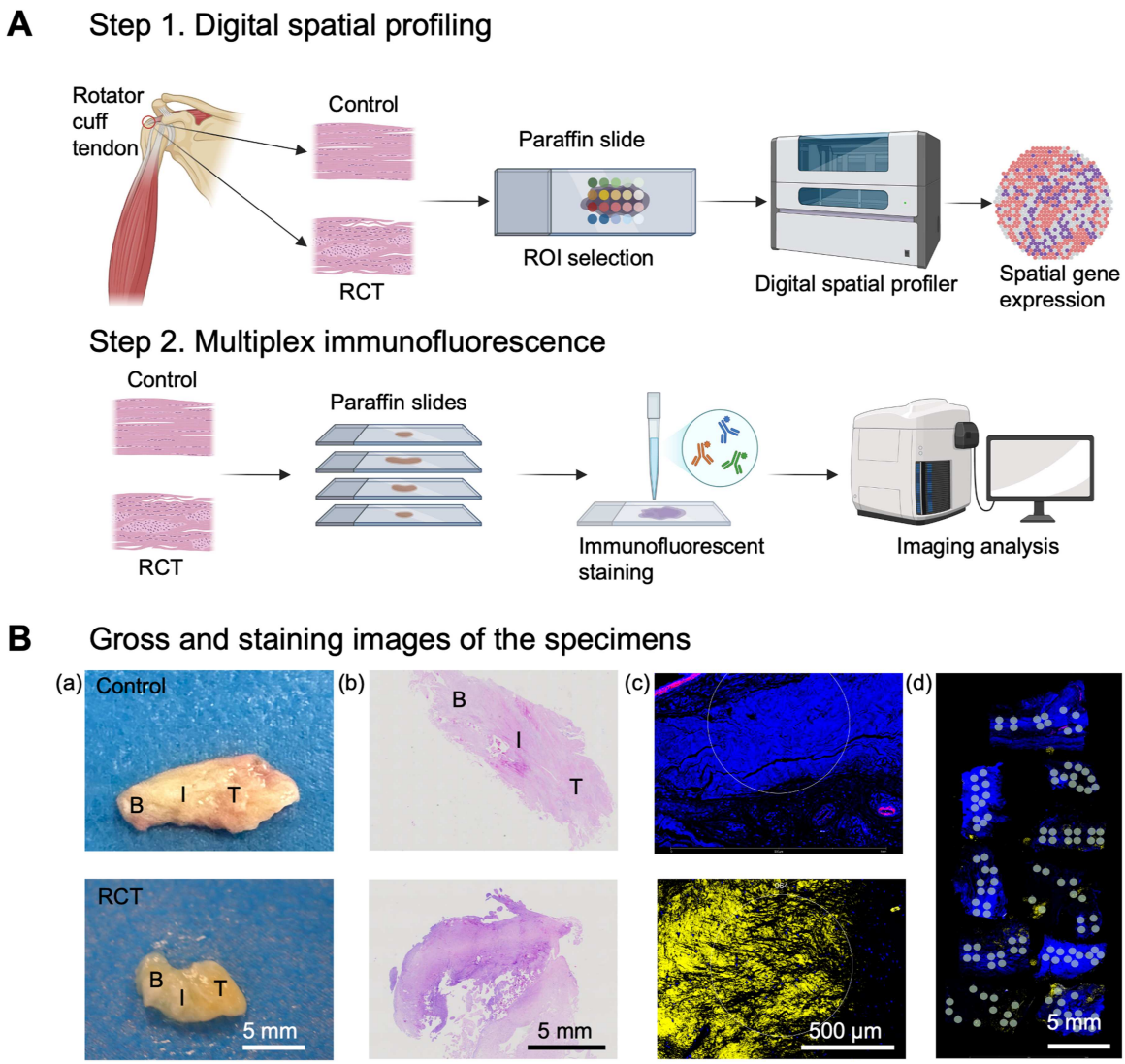

FIGURE 1 | Schematic diagram of the experimental design and the condition of the specimens. (A) The two steps of the experiment. (B) Gross (a) and staining (b–d) images of the specimens. B, bone part; I, middle part; T, tendon part.

structure of the RCT group appeared loose, with disordered fibers and cells in the HE sections (Figure 1B(b)). Fluorescent staining revealed a significant infiltration of inflammatory cells (CD68, yellow fluorescence; DAPI, blue fluorescence) (Figure 1B(c)). Figure 1B(d) shows the ROIs of the specimens that we have selected for analysis.

3.2 | Differential Gene Analysis

The principal component analysis (PCA) of the detected transcripts indicated that the RCT tissue exhibited a distinct clustering pattern compared to the control group, with some degree of overlap. Upon segmenting the tissue into three components—the bone part (B), the middle part (I), and the tendon part (T)—differences among these sections were also observed based on the overlapping data (Figure 2A). In comparison to the RCT group, the control group displayed 1261 down-regulated genes and 2789 up-regulated genes. Spatial analysis revealed a clear yet overlapping expression gradient in the control tendon: COMP and CHI3L1 were up-regulated in the bone part, CHI3L1 and MT1X were up-regulated in the middle part, and MT1X and FMOD were up-regulated in the tendon part (Figure 2B).

3.3 | The Biological Processes and Signaling Pathways

The differential gene expression profiles in each segment led to the enrichment of distinct pathological biological processes associated with specific signaling pathways and their interplays. Key genes were consistently expressed within these pathways. In the bone region, the predominant processes involved cartilage development and extracellular matrix organization (Figure 3A), governed mainly by the PI3K-Akt signaling pathway and ECM-receptor interaction (Figure 3B). In the middle segment, key processes included collagen fibril organization and extracellular matrix organization (Figure 4A), with the same pathways—PI3K-Akt and ECM-receptor interaction—playing central roles (Figure 4B). In the tendon part, the predominant influences were again collagen fibril organization and extracellular matrix organization (Figure 5A), with the

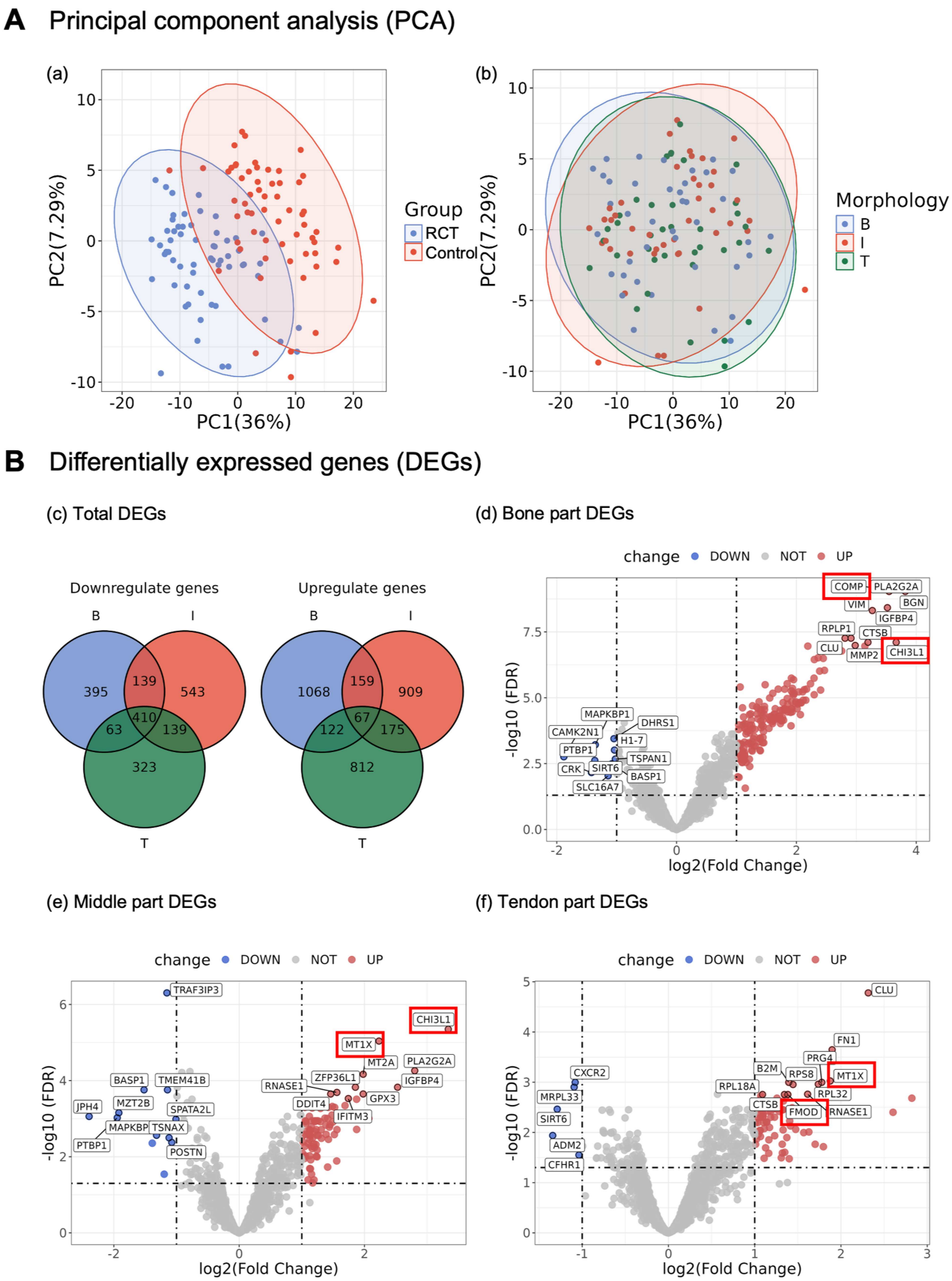

FIGURE 2 | Principal component analysis (PCA) and differentially expressed genes (DEGs). (A) PCA analysis between the two groups (a) and the three parts (b). (B) Total DEGs and DEGs in the three parts (b–d). B, bone part; I, middle part; T, tendon part; "up" refers to control samples; "down" refers to RCT samples.

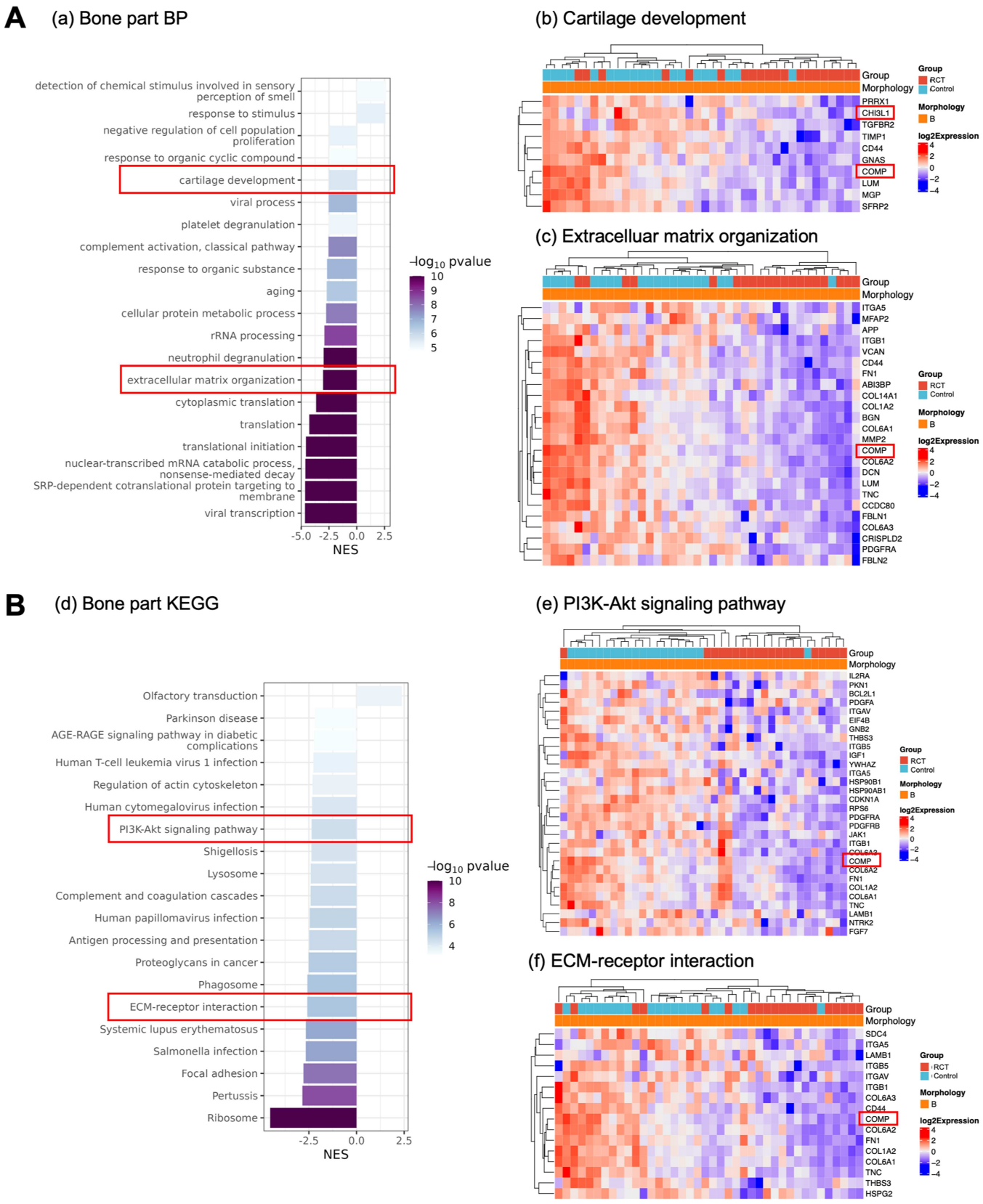

FIGURE 3 | Biological processes (BPs) and KEGG enrichment pathways in the bone part. (A) The main BPs (a) and the two prominent ones (b, c). (B) The main KEGGs (d) and the two prominent ones (e, f).

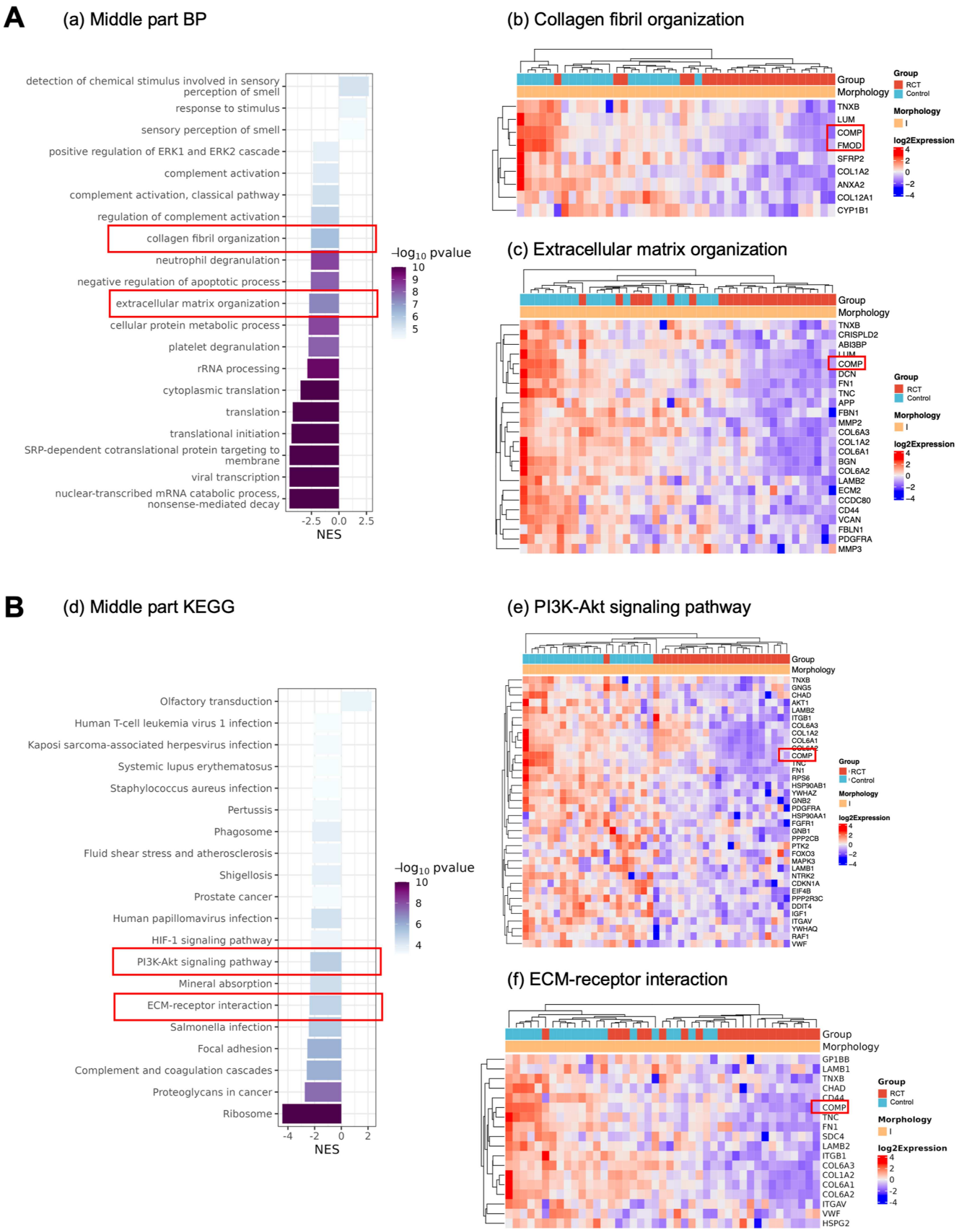

FIGURE 4 | Biological process (BP) and KEGG enrichment pathways in the middle part. (A) The main BPs (a) and the two prominent ones (b, c). (B) The main KEGGs (d) and the two prominent ones (e, f).

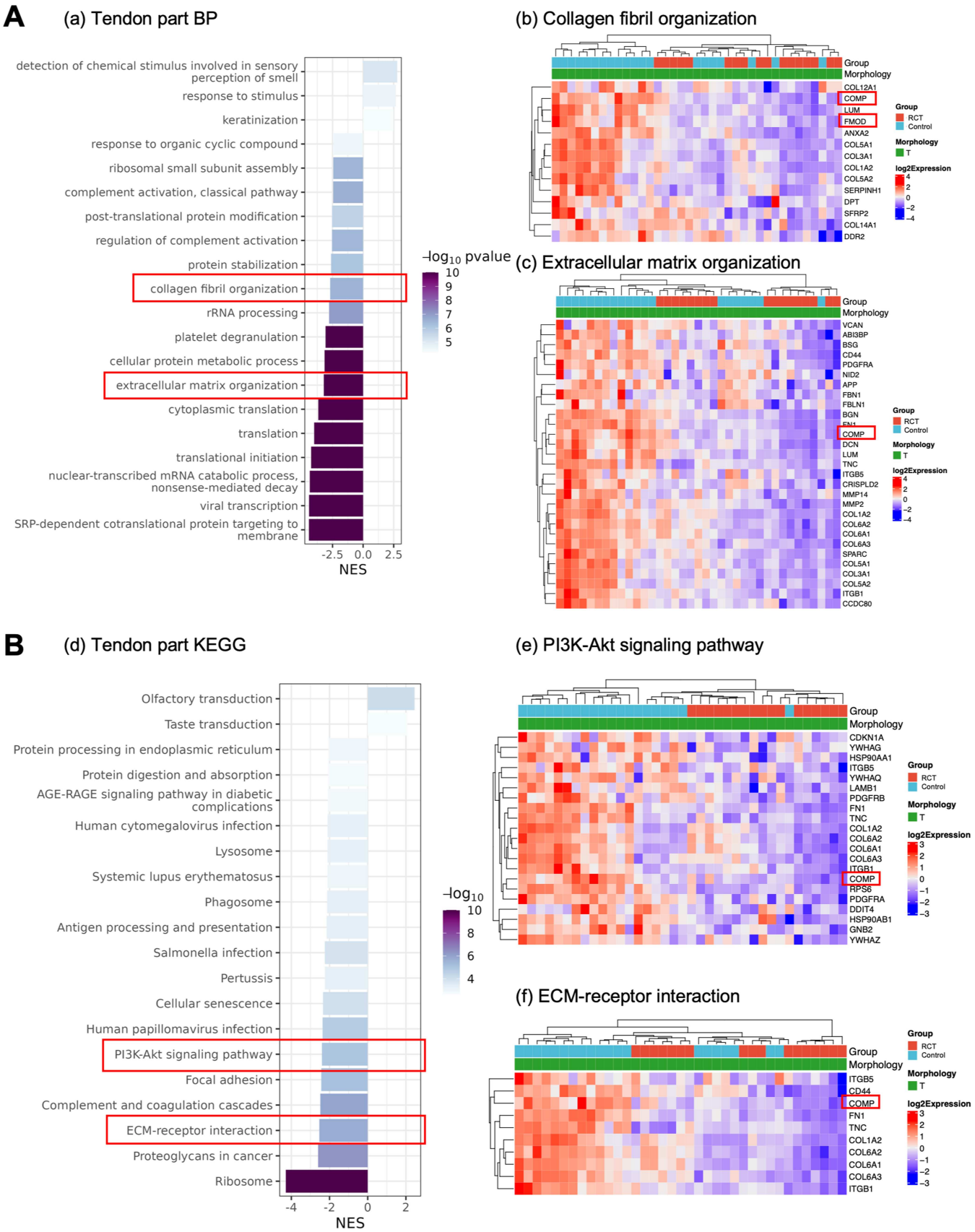

FIGURE 5 | Biological process (BP) and KEGG enrichment pathways in the tendon part. (A) The main BPs (a) and the two prominent ones (b, c). (B) The main KEGGs (d) and the two prominent ones (e, f).

corresponding signaling pathways remaining the PI3K-Akt signaling pathway and ECM-receptor interaction (Figure 5B).

3.4 | mIF Verification

Furthermore, to verify the distribution and intuitive expression of key genes in the tissue sections, we employed the mIF method for immunofluorescence staining. The tissue section slides from the RCT group exhibited slightly inferior quality compared to those from the control group (Figure 6A). The staining intensity of each protein in the control group was stronger than that in the RCT group, specifically for CHI3L1 (red), COMP (green), FMOD (orange), and MT1X (cyan) (Figure 6B,C).

3.5 | Cell Changes in Each Part

We utilized the CIBERSORT method to infer the cell composition involved within the study area based on the expression data from the scRNA datasets (GSE223751, GSE182997), focusing on observing tendon fibroblasts, tenogenic progenitor-like cells, mesenchymal cells, macrophages, and so forth. (Figure 7A). Table 3 shows the markers used when labeling these cells. Among them, the number of tenogenic progenitor-like cells in the control group was significantly higher than that in the RCT group ($p < 0.0001$) (Figure 7B). From each part, the number of mesenchymal cells in the bone part and the middle part was significantly higher than that in the control group ($p < 0.001$, $p < 0.01$, respectively). However, in the tendon part, there was no significant difference in the number of mesenchymal cells. These changes presented the characteristic gradient changes and regenerative features of this location.

4 | Discussion

This study identified four key genes (COMP, CHI3L1, MT1X, and FMOD) by analyzing the differentially expressed genes in RCT and control tissues. The results indicate that these genes are closely associated with cartilage development, collagen fibril organization, and extracellular matrix organization functions, as well as the PI3K-AKT signaling pathway, ECM-receptor interaction pathway, and the regulation of TPLC and mesenchymal cell functions. These findings offer a new perspective for understanding the molecular mechanisms underlying RCT.

4.1 | The Function of Key Genes

4.1.1 | Cartilage Oligomeric Matrix Protein (COMP)

COMP is a non-collagenous extracellular matrix glycoprotein primarily found in the human skeletal system, including articular cartilage, meniscus, ligaments, tendons, and synovium [17, 18]. It plays a crucial role in the ECM homeostasis [19]. Abnormal expression of this protein can lead to a disordered arrangement of collagen fibers [20], which may adversely affect the properties of the tissue, similar to the condition observed in RCT.

4.1.2 | Chitinase 3-like Protein 1 (CHI3L1)

CHI3L1 is a secreted glycoprotein that has been shown in recent studies to play a significant role in cartilage metabolism, inflammatory responses, and tissue repair [21]. The subpopulation of cartilage cells expressing CHI3L1 is believed to be associated with the stability of cell microtubules, which may serve as a potential mechanism for cartilage regeneration and repair [22]. This makes CHI3L1 a promising target for the treatment of cartilage injuries, which may also have therapeutic effects on the bone part of the RCT.

4.1.3 | Metallothionein 1X (MT1X)

MT1X is a type of metal-binding protein, mainly involved in metal ion homeostasis, antioxidant stress, and cellular protection. Specifically, the upregulation of MT1X is regarded as a beneficial factor for extending lifespan, as it exerts a more substantial regulatory effect on zinc homeostasis [23]. In the damaged tendons, the expression level of MT1X is decreased, suggesting that the metal homeostasis may be disrupted, which could contribute to tendon degeneration [24]. The tendon degeneration may also be associated with changes in the MT1X protein, which has been identified as an age-related gene in RCTs in another study [24].

4.1.4 | Fibromodulin (FMOD)

FMOD is a small leucine-rich glycoprotein that is mainly found in the ECM, particularly within connective tissues such as tendons [25]. It plays a vital role in preserving tissue structure and function by regulating the assembly and stability of collagen fibers. Among the RCTs classified as small, medium, large, and massive, the small-sized RCTs had the highest retention rate of FMOD [7]. The combination of COL1 and FMOD represents the primary active molecules in the extracellular matrix of tendon cells, likely influencing the differentiation of tendon cells and holding significant potential for tendon engineering applications [26].

4.2 | Pathways and Pathological Mechanisms

The activation of the PI3K-AKT pathway may participate in the process of RCT by regulating cell proliferation, apoptosis, and metabolism [27]. In a neonatal mouse model of Achilles tendon rupture, inhibition of the PI3K-AKT signaling pathway decreases the proliferation and migration of Scx tendon cells [28]. Furthermore, inhibiting the PI3K-AKT signaling pathway diminishes the stemness of Scx tendon cells.

The enrichment of the ECM-receptor interaction pathway further emphasizes the central role of ECM imbalance [29], which is consistent with the imbalance of the expression of MMPs and ADAMs reported in a previous study [9]. Abnormalities in genes such as COMP and FMOD may exacerbate tendon degeneration through the integrin-ECM feedback loop [30]. This pathway may provide a theoretical foundation for therapeutic strategies aimed at targeting ECM remodeling.

4.3 | Distribution and Function of Cells Involved

The differences in the expression of TPLCs and mesenchymal cells suggest that local cell dysfunction may be involved in the

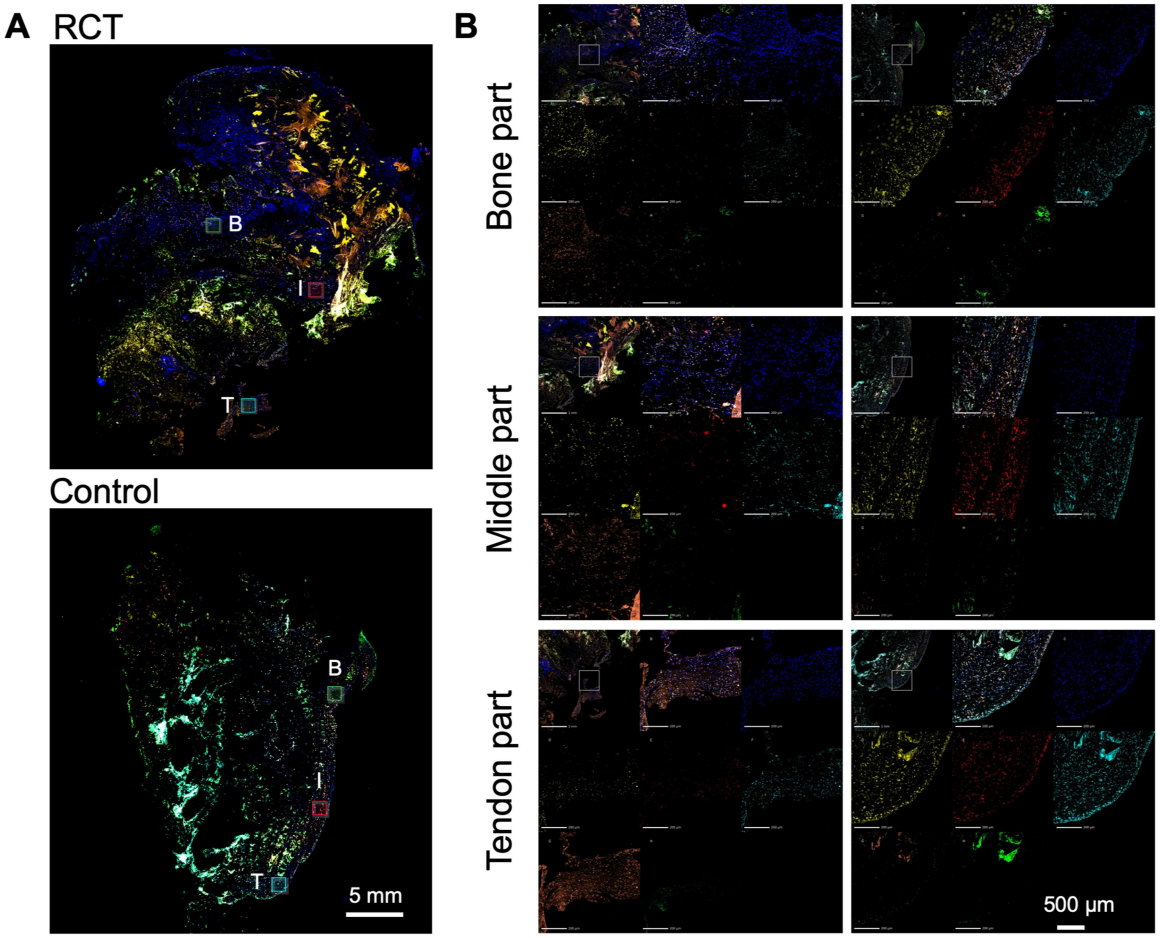

C

CHI3L1	Opal 690	Red
COMP	Opal 520	Green
FMOD	Opal 620	Orange
MT1X	Opal 480	Cyan

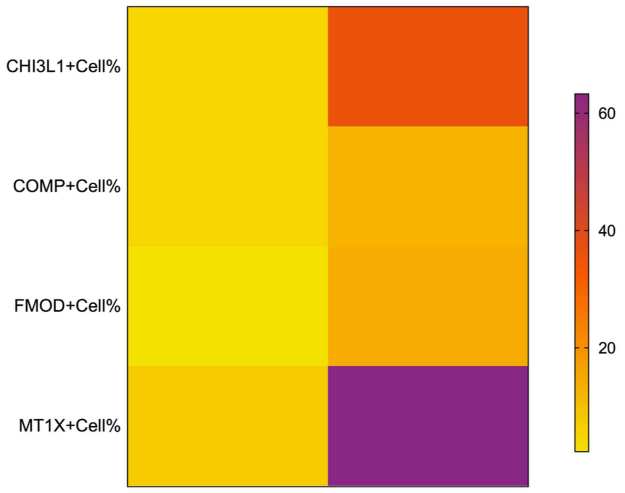

FIGURE 6 | Multiplex immunofluorescence (mIF) staining and relative quantification of the tissues. (A) mIF images between groups. (B) mIF images in the three parts. (C) Relative quantification of the positively stained cells. B, bone part; I, middle part; T, tendon part.

pathological process of RCT. During the healing process of the rotator cuff tendon-bone junction, TPLCs [31] and mesenchymal cells [32] work synergistically to promote repair through distinct distribution patterns. TPLCs mainly accumulate at the tendon end, where they secrete growth factors such as TGF-β and IGF-1 to facilitate the regeneration of the fibrocartilage band and differentiate into tendon cells, thereby enhancing the integration of tendon tissue [33]. In contrast, mesenchymal cells tend to cluster at the bone interface, accelerating bone callus formation through osteogenic differentiation (characterized by the upregulation of Runx2, Osterix expression) and angiogenic effects (VEGF secretion) while also regulating the local inflammatory microenvironment [34]. This spatiotemporal specific distribution and functional complementarity optimize

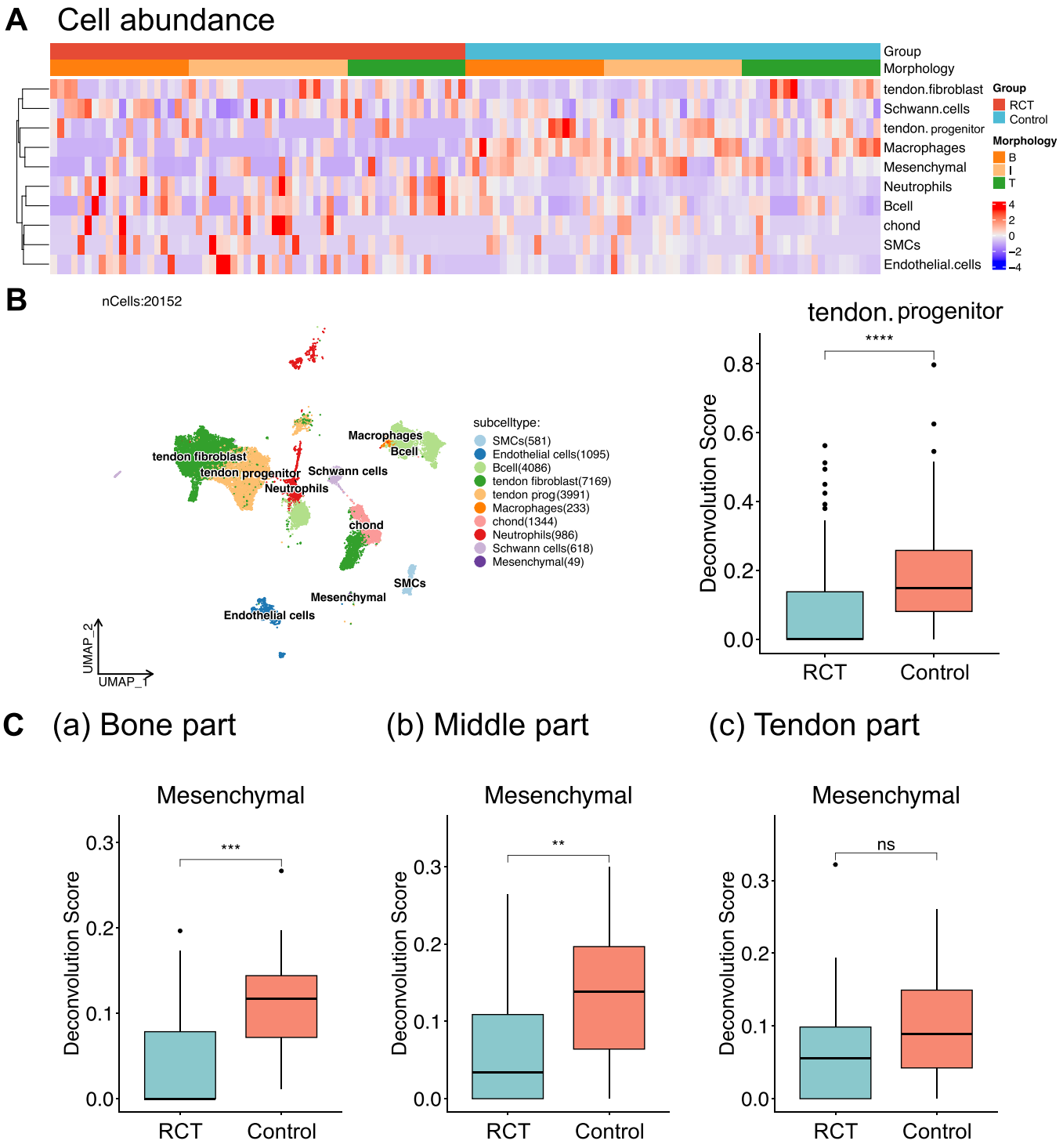

FIGURE 7 | Cell interpretation in the tissue. (A) The main cell types that influence the rotator cuff quality. (B) Differences in the tenogenic progenitor-like cells between groups. (C) Differences in the mesenchymal cells in the three parts between groups.

the reconstruction of the gradient structure at the tendon-bone interface, providing a theoretical basis for clinical cell-targeted therapies.

5 | Conclusion and Limitations

Spatial transcriptomics analysis and mIF revealed the molecular characteristics of RCT in the elderly, including increased inflammation, ECM degradation, and reduced regenerative capacity. The limitations of this study include a small sample size, the ethical difficulties in obtaining normal human tendon samples, the lack of comprehensive, well-annotated human tendon single-cell RNA-seq references (better annotated in the paper published by Fu et al. [11]), and the absence of functional experimental validation. Future research should clarify the causal roles of the identified genes and cell-cell interactions among identified cell

TABLE 3 | The detailed markers used for cell annotation.

Cell type	Markers
Schwann cells	Mpz, Pmp22
SMCs	Tagln, Acta2, Myh11
Macrophages	CD14, CD68
Neutrophils	S100a8, S100a9
Endothelial cells	Cdh5, Pecam1
B cells	Cd19, Cd79a, Cd79b, Ms4a1
Mesenchymal cells	Pdgfrb, Fap
Chondrocytes	Acan, Sox9, Col2a1
Tendon fibroblasts	Tnmd, Fmod, Thbs4
Tendon progenitor-like cells	Fbn1, Mfap5, Ly6a

populations. Furthermore, targeted interventions, such as small-molecule inhibitors or gene therapies, for key genes and pathways warrant further investigation.

Author Contributions

Experimental design: Shiyi Yao and Lei Wang. Data acquisition and analysis: Shifeng Ling. Figure preparation: Gen Li and Hanyu Wang. RNA-Seq analysis: Renxuan Li and Yang Xu. Manuscript writing: Shiyi Yao, Yin Zhang, and Chengyu Zhuang.

Acknowledgments

This work was funded by the National Natural Science Foundation of China (Grant No. 82402784, 82472419), the Postdoctoral Science Foundation General Program (2024M762056).

Ethics Statement

This retrospective study received approval from the Ethics Committee of Ruijin Hospital, Shanghai Jiao Tong University School of Medicine (Shanghai, China; No. 2024-53). All donors provided written informed consent for the use of their excised rotator cuff tissue. They were fully informed about the purpose of the research, and no compensation was offered for their donations.

Conflicts of Interest

The authors declare no conflicts of interest.

Data Availability Statement

The data that support the findings of this study are available from the corresponding author upon reasonable request.

References

1. A. Bedi, J. Bishop, J. Keener, et al., "Rotator Cuff Tears," *Nature Reviews Disease Primers* 10, no. 1 (2024): 8, https://doi.org/10.1038/s41572-024-00492-3.

2. G. L. Cvetanovich, B. R. Waterman, N. N. Verma, and A. A. Romeo, "Management of the Irreparable Rotator Cuff Tear," *Journal of the American Academy of Orthopaedic Surgeons* 27, no. 24 (2019): 909–917, https://doi.org/10.5435/JAAOS-D-18-00199.

3. C. A. Kwong, Y. Ono, M. J. Carroll, et al., "Full-Thickness Rotator Cuff Tears: What is the Rate of Tear Progression? A Systematic Review," *Arthroscopy: The Journal of Arthroscopic and Related Surgery* 35, no. 1 (2019): 228–234, https://doi.org/10.1016/j.arthro.2018.07.031.

4. F. H. Savoie Iii, B. P. Delvadia, J. P. Tate, et al., "Biologics in Rotator Cuff Repair," *Bone and Joint Journal* 106–B, no. 9 (2024): 978–985, https://doi.org/10.1302/0301-620X.106B9.BJJ-2024-0513.R1.

5. J. Zhao, M. Luo, J. Pan, et al., "Risk Factors Affecting Rotator Cuff Retear After Arthroscopic Repair: A Meta-Analysis and Systematic Review," *Journal of Shoulder and Elbow Surgery* 30, no. 11 (2021): 2660–2670, https://doi.org/10.1016/j.jse.2021.05.010.

6. J. D. Keener, B. M. Patterson, N. Orvets, and A. M. Chamberlain, "Degenerative Rotator Cuff Tears: Refining Surgical Indications Based on Natural History Data," *Journal of the American Academy of Orthopaedic Surgeons* 27, no. 5 (2019): 156–165, https://doi.org/10.5435/JAAOS-D-17-00480.

7. J. Jiang, K. H. Jang, S. Y. Ahn, and C. H. Jo, "Changes in Gene Expression of the Extracellular Matrix in Patients With Full-Thickness Rotator Cuff Tears of Varying Sizes," *Clinics in Orthopedic Surgery* 17, no. 1 (2025): 138–147, https://doi.org/10.4055/cios24125.

8. R. Z. Tashjian, S. K. Kim, M. D. Roche, K. B. Jones, and C. C. Teerlink, "Genetic Variants Associated With Rotator Cuff Tearing Utilizing Multiple Population-Based Genetic Resources," *Journal of Shoulder and Elbow Surgery* 30, no. 3 (2021): 520–531, https://doi.org/10.1016/j.jse.2020.06.036.

9. S. Chaudhury, Z. Xia, D. Thakkar, O. Hakimi, and A. J. Carr, "Gene Expression Profiles of Changes Underlying Different-Sized Human Rotator Cuff Tendon Tears," *Journal of Shoulder and Elbow Surgery* 25, no. 10 (2016): 1561–1570, https://doi.org/10.1016/j.jse.2016.02.037.

10. R. Z. Tashjian, I. Lock, E. K. Granger, et al., "Gene Expression in Torn Rotator Cuff Tendons Determined by RNA Sequencing," *Orthopaedic Journal of Sports Medicine* 8, no. 6 (2020): 2325967120927480, https://doi.org/10.1177/2325967120927480.

11. W. Fu, R. Yang, and J. Li, "Single-Cell and Spatial Transcriptomics Reveal Changes in Cell Heterogeneity During Progression of Human Tendinopathy," *BMC Biology* 21, no. 1 (2023): 132, https://doi.org/10.1186/s12915-023-01613-2.

12. C. R. Merritt, G. T. Ong, S. E. Church, et al., "Multiplex Digital Spatial Profiling of Proteins and RNA in Fixed Tissue," *Nature Biotechnology* 38, no. 5 (2020): 586–599, https://doi.org/10.1038/s41587-020-0472-9.

13. L. Brady, M. Kriner, I. Coleman, et al., "Inter- and Intra-Tumor Heterogeneity of Metastatic Prostate Cancer Determined by Digital Spatial Gene Expression Profiling," *Nature Communications* 12, no. 1 (2021): 1426, https://doi.org/10.1038/s41467-021-21615-4.

14. J. P. Väyrynen, "Multiplex Immunofluorescence for Tumour Immune Biomarker Discovery," *Lancet Oncology* 25, no. 2 (2024): 151–152, https://doi.org/10.1016/S1470-2045(23)00583-1.

15. W. C. C. Tan, S. N. Nerurkar, H. Y. Cai, et al., "Overview of Multiplex Immunohistochemistry/Immunofluorescence Techniques in the Era of Cancer Immunotherapy," *Cancer Communications* 40, no. 4 (2020): 135–153, https://doi.org/10.1002/cac2.12023.

16. M. D. Robinson and A. Oshlack, "A Scaling Normalization Method for Differential Expression Analysis of RNA-Seq Data," *Genome Biology* 11, no. 3 (2010): R25, https://doi.org/10.1186/gb-2010-11-3-r25.

17. C. Li, N. Wang, A. A. Schäffer, et al., "Mutations in COMP Cause Familial Carpal Tunnel Syndrome," *Nature Communications* 11, no. 1 (2020): 3642, https://doi.org/10.1038/s41467-020-17378-z.

18. M. López-Franco, O. López-Franco, M. A. Murciano-Antón, et al., "Meniscal Degeneration in Human Knee Osteoarthritis: In Situ Hybridization and Immunohistochemistry Study," *Archives of Orthopaedic and Trauma Surgery* 136, no. 2 (2016): 175–183, https://doi.org/10.1007/s00402-015-2378-4.

19. K. L. Posey, F. Coustry, and J. T. Hecht, "Cartilage Oligomeric Matrix Protein: Compopathies and Beyond," *Matrix Biology* 71–72 (2018): 161–173, https://doi.org/10.1016/j.matbio.2018.02.023.

20. Y. Xiong, X. Li, B. Sun, J. Zhang, X. Wu, and F. Guo, "Abnormal Collagen Deposition Mediated by Cartilage Oligomeric Matrix Protein in the Pathogenesis of Oral Submucous Fibrosis," *International Journal of Oral Science* 17, no. 1 (2025): 25, https://doi.org/10.1038/s41368-025-00355-x.

21. L. Li, K. Wei, Y. Ding, et al., "M2a Macrophage-Secreted CHI3L1 Promotes Extracellular Matrix Metabolic Imbalances via Activation of IL-13Ralpha2/MAPK Pathway in Rat Intervertebral Disc Degeneration," *Frontiers in Immunology* 12 (2021): 666361, https://doi.org/10.3389/fimmu.2021.666361.

22. J. Li, C. Fan, Z. Lv, et al., "Microtubule Stabilization Targeting Regenerative Chondrocyte Cluster for Cartilage Regeneration," *Theranostics* 13, no. 10 (2023): 3480–3496, https://doi.org/10.7150/thno.85077.

23. R. Giacconi, L. Costarelli, F. Piacenza, et al., "Zinc-Induced Metallothionein in Centenarian Offspring From a Large European Population: The MARK-AGE Project," *Journals of Gerontology: Series A* 73, no. 6 (2018): 745–753, https://doi.org/10.1093/gerona/glx192.

24. Y. Liu, X. Li, L. Jiang, and J. Ma, "Identification of Age-Related Genes in Rotator Cuff Tendon," *Bone and Joint Research* 13, no. 9 (2024): 474–484, https://doi.org/10.1302/2046-3758.139.BJR-2023-0398.R1.

25. X. Xu, Y. Zhang, P. Ha, et al., "A Novel Injectable Fibromodulin-Releasing Granular Hydrogel for Tendon Healing and Functional Recovery," *Bioengineering and Translational Medicine* 8, no. 1 (2023): e10355, https://doi.org/10.1002/btm2.10355.

26. T. Tu, Y. Shi, B. Zhou, et al., "Type I Collagen and Fibromodulin Enhance the Tenogenic Phenotype of hASCs and Their Potential for Tendon Regeneration," *NPJ Regenerative Medicine* 8, no. 1 (2023): 67, https://doi.org/10.1038/s41536-023-00341-z.

27. Z. Zhang, Y. Zhang, H. Wang, et al., "Curcumin Improves Functional Recovery of Ruptured Tendon by Promoting Tenogenesis via PI3K/Akt Signaling," *Stem Cells Translational Medicine* 13, no. 5 (2024): 477–489, https://doi.org/10.1093/stcltm/szae007.

28. A. Goto, S. Komura, K. Kato, et al., "PI3K-Akt Signalling Regulates Scx-Lineage Tenocytes and Tppp3-lineage Paratenon Sheath Cells in Neonatal Tendon Regeneration," *Nature Communications* 16, no. 1 (2025): 3734, https://doi.org/10.1038/s41467-025-59010-y.

29. K. Xu, Y. Shao, Y. Xia, et al., "Tenascin-Cregulates Migration of SOX10 Tendon Stem Cells via Integrin-α9 for Promoting Patellar Tendon Remodeling," *Biofactors* 47, no. 5 (2021): 768–777, https://doi.org/10.1002/biof.1759.

30. A. S. Yatsenko and H. R. Shcherbata, "Drosophila miR-9a Targets the ECM Receptor Dystroglycan to Canalize Myotendinous Junction Formation," *Developmental Cell* 28, no. 3 (2014): 335–348, https://doi.org/10.1016/j.devcel.2014.01.004.

31. Z. Chen, P. Chen, M. Zheng, et al., "Challenges and Perspectives of Tendon-Derived Cell Therapy for Tendinopathy: From Bench to Bedside," *Stem Cell Research and Therapy* 13, no. 1 (2022): 444, https://doi.org/10.1186/s13287-022-03113-6.

32. Z. Wang, Y. Liao, C. Wang, et al., "Stem Cell-Based Therapeutic Strategies for Rotator Cuff Tendinopathy," *Journal of Orthopaedic Translation* 42 (2023): 73–81, https://doi.org/10.1016/j.jot.2023.07.006.

33. S. Shen, Y. Lin, J. Sun, Y. Liu, Y. Chen, and J. Lu, "A New Tissue Engineering Strategy to Promote Tendon-Bone Healing: Regulation of Osteogenic and Chondrogenic Differentiation of Tendon-Derived Stem Cells," *Orthopaedic Surgery* 16, no. 10 (2024): 2311–2325, https://doi.org/10.1111/os.14152.

34. J. Zhang, J. Pan, and W. Jing, "Motivating Role of Type H Vessels in Bone Regeneration," *Cell Proliferation* 53, no. 9 (2020): e12874, https://doi.org/10.1111/cpr.12874.